

## Octupole Deformation in Neutron-Rich Barium Isotopes

W. R. Phillips,<sup>(a)</sup> I. Ahmad, H. Emling,<sup>(b)</sup> R. Holzmann, R. V. F. Janssens, and T.-L. Khoo  
*Argonne National Laboratory, Argonne, Illinois 60439*

and

M. W. Drigert  
*University of Notre Dame, Notre Dame, Indiana 46556*  
 (Received 6 October 1986)

Partial decay schemes for the very neutron-rich nuclei  $^{142,144}\text{Ba}$  and  $^{146}\text{Ba}$  have been determined by the study of  $\gamma$ - $\gamma$  coincidences in  $^{252}\text{Cf}$  fission fragments. Interlaced positive- and negative-parity levels connected by fast electric dipole transitions are observed in  $^{144}\text{Ba}$  and  $^{146}\text{Ba}$  above spin  $7\hbar$ . This is similar to the situation in some light actinide nuclei, where the data have been interpreted in terms of reflection-asymmetric shapes.

PACS numbers: 21.10.Re, 23.20.Lv, 25.85.Ca, 27.60.+j

The recent discoveries<sup>1-4</sup> in light actinide nuclei of level patterns similar to rotational bands in reflection-asymmetric molecules suggest that some nuclei at moderate spin have stable shapes which may incorporate octupole deformation. This possibility has been examined for some time but received renewed attention in view of the observations on the light Ac, Ra, and Th nuclei. In the even-even isotopes, as the spin increases, negative- and positive-parity levels become interlaced with spacings roughly appropriate to a single band. The levels in these bands are connected by both strong electric quadrupole and strong electric dipole transitions. These data have been interpreted<sup>5,6</sup> in terms of an axially symmetric octupole deformation which stabilizes as the nuclear rotation increases. Other interpretations have also been proposed including one<sup>7</sup> in the interacting-boson-model framework and one which uses a molecular-cluster model.<sup>8</sup>

Only in restricted regions of the nuclear chart are nuclei expected to gain appreciable amounts of binding energy by assumption of octupole deformations. These regions occur when a pair of single-particle orbitals with  $\Delta l = 3$  and  $\Delta j = 3$  having large octupole-interaction matrix elements lies close to each other. Detailed mean-field calculations<sup>9</sup> for ground states predict that octupole deformations are most likely near  $A = 224$ , with  $Z \sim 90$  and  $N \sim 134$ , and in a region near  $Z = 56$ ,  $N = 90$ . Structures suggestive of octupole deformation have been reported near  $A = 224$ , and it is of great interest to examine the second group to test the predictions and to explore similarities with those near  $A = 224$ .

There is very little information on nuclei near  $Z = 56$ ,  $N = 90$  at spins higher than a few units: They are very neutron-rich and are not accessible with the usual in-beam techniques. They are, however, some of the most copious products of the spontaneous fission of  $^{252}\text{Cf}$ , and this Letter reports partial decay paths for discrete levels in  $^{142,144}\text{Ba}$  and  $^{146}\text{Ba}$  populated following statistical de-

decay of primary fission fragments. Some levels at low excitation energy and spin in the relevant Ba isotopes have been determined from previous studies of  $^{252}\text{Cf}$  decay products<sup>10</sup> and decays of Cs isotopes.<sup>11</sup> The average spin<sup>12</sup> in a final Ba fragment is about  $5\hbar$  and high sensitivity is needed to observe higher-spin discrete levels which become more weakly populated and whose decay  $\gamma$  rays sit on a background of very many lines from other fission fragments. The required sensitivity was obtained by use of seven bismuth-germanate-suppressed Ge detectors of the Argonne-Notre Dame  $\gamma$ -ray facility and one LEPS (low-energy photon spectrometer) detector for x rays and low-energy  $\gamma$  rays, all in prompt coincidence with each other. A further requirement for events analyzed was that a coincident signal occurred in at least one of fourteen bismuth germanate detectors of a multiplicity array located close to the source. The triple coincidence requirement eliminated most beta-decay backgrounds and emphasized prompt events of high multiplicity.

A  $60\text{-}\mu\text{Ci}$   $^{252}\text{Cf}$  source was embedded in a Be cylinder which had an  $8\text{-mg-cm}^{-2}$ -thick front face through which x rays could emerge. The Ba fragments slow down in Be in about 2 ps and mainly emit  $\gamma$  rays at rest. The main discrete line pathways were determined in the usual way from the analysis of  $\gamma$ - $\gamma$  and  $\gamma$ -LEPS coincidence data. In most cases it was possible to place  $\gamma$  rays in decay schemes as long as their intensities were greater than about one percent of that of the  $^{144}\text{Ba}$   $2_1^+ \rightarrow 0_1^+$  line, which is present in  $\sim 3.5\%$  of the fission decays of  $^{252}\text{Cf}$ .

Figure 1 shows the schemes obtained. They are the most extensive available for nuclei with a large neutron excess. No simple feeding pattern was seen in  $^{142}\text{Ba}$ . In  $^{144}\text{Ba}$  the discrete levels observed comprise two sets of states with strong sideways transitions between them. These transitions were established to be  $E1$ , and hence  $(I+1) \rightarrow I$ , on the basis of the following observations: (i) Legendre polynomial fits to  $\gamma$ - $\gamma$  angular correlations

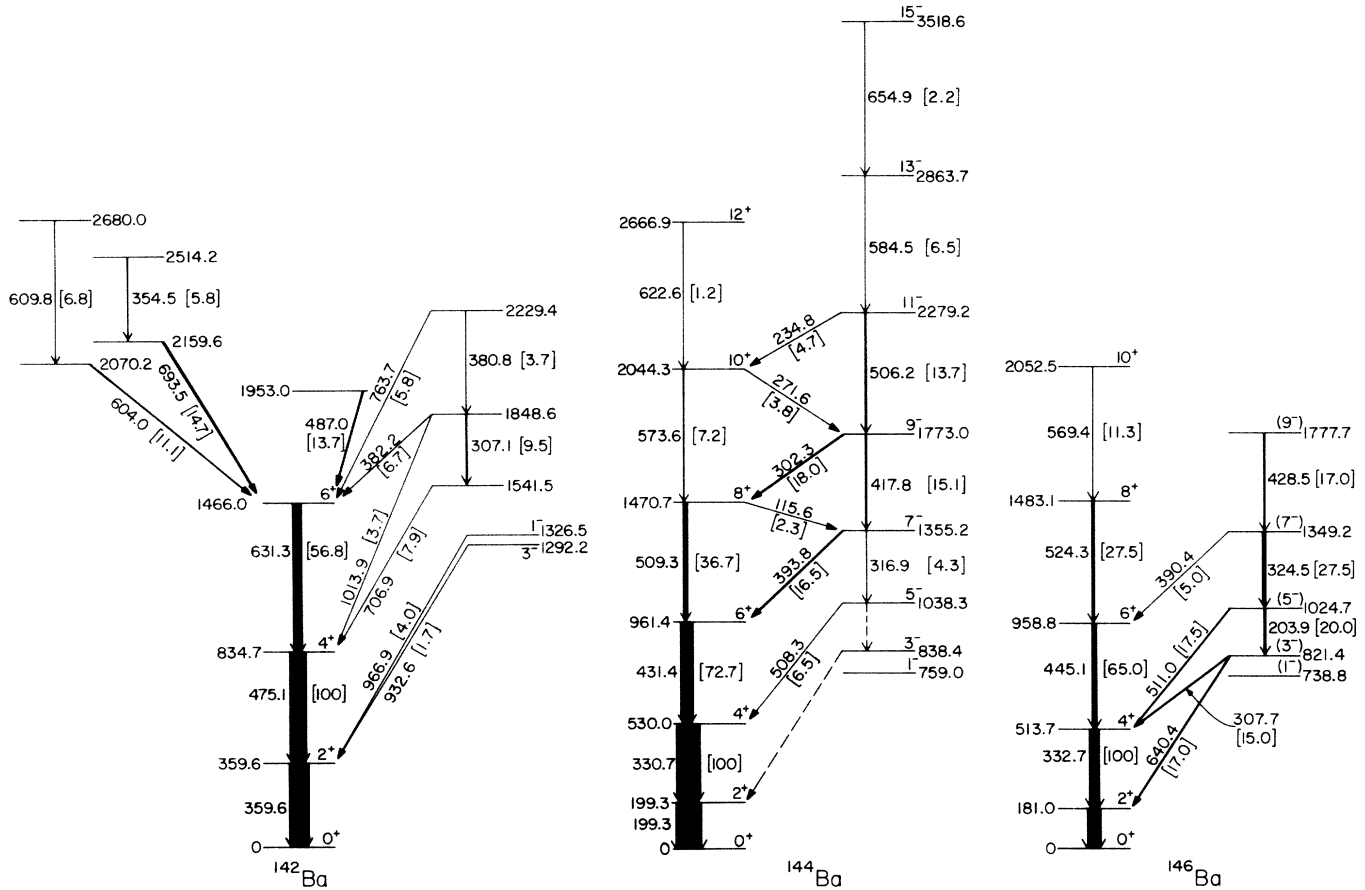


FIG. 1. Partial decay schemes for  $^{142-146}\text{Ba}$ . The numbers in square brackets are the relative intensities of  $\gamma$  rays in coincidence with the  $2_1^+ \rightarrow 0_1^+$   $\gamma$  ray in each nucleus. The errors on the relative intensities vary from  $\sim 25\%$  for the weak  $\gamma$  rays to  $\sim 5\%$  for the most intense. The measured populations of  $^{142}\text{Ba}$ ,  $^{144}\text{Ba}$ , and  $^{146}\text{Ba}$  were in the ratios 0.68:1.00:0.29. The errors on the level energies and  $\gamma$ -ray energies are 0.2 keV or better; there is an additional uncertainty of 0.2 keV on the absolute energies.

gave the mean value of the coefficient  $A_2$  of 0.07(2) for the strong in-band cascades in the even Ba isotopes, consistent with the prediction of 0.10 for stretched  $E2-E2$  correlations. For the strongest  $(I+1) \rightarrow I$  transitions in  $^{144}\text{Ba}$  the mean value was  $-0.01(5)$ , consistent with the prediction of  $-0.014$  for stretched dipole-quadrupole correlations. (ii) The  $K$ -conversion coefficient  $\alpha_K$  for the 116-keV  $\gamma$  ray in  $^{144}\text{Ba}$  was measured from LEPS spectra in coincidence with the 431- and 394-keV  $\gamma$  rays. The relative intensities of the 116-keV  $\gamma$  ray and of the Ba  $K\alpha$  x ray (after subtraction of contributions from other transitions) gave a weighted mean value for  $\alpha_K$  of 0.16(30). The theoretical values are 0.13 for  $E1$ , 0.6 for  $M1$ , and 0.75 for  $E2$ . (iii) The reduced transition probabilities  $B(\lambda)$  for the sideways transitions were estimated from the relative  $\gamma$ -ray intensities for different assumed multipolarities with use of the measured<sup>13</sup> intrinsic quadrupole moment. If they are  $E1$ , their average strength is  $\sim 10^{-3}$  Weisskopf units (W.u.); if  $M1$  it is  $\sim 10^{-1}$  W.u. There are no known interband  $M1$  transitions in medium- $A$  even nuclei with strengths of this

magnitude.<sup>14</sup> The weight of all the evidence points to  $E1$  character for the sideways  $\gamma$  rays. Their  $B(E1)$  values are given in Table I.

Levels in  $^{146}\text{Ba}$  were not identified to spins as high as in  $^{144}\text{Ba}$ , mainly because  $^{146}\text{Ba}$  is populated about 4 times less in the fission of  $^{252}\text{Cf}$ . In  $^{146}\text{Ba}$  the discrete levels observed again comprise two sets. One set includes known<sup>12</sup> levels of spins 1 and 3, and strong  $\gamma$  rays are observed from the levels of assumed spins 5 and 7 to the  $4_1^+$  and  $6_1^+$  levels. The assignments of odd parity and spin to levels in  $^{146}\text{Ba}$  are not as certain as in  $^{144}\text{Ba}$ . However, it is very likely by analogy with  $^{144}\text{Ba}$  that the set containing the spin-1 and spin-3 levels has odd spins and negative parity and that the  $\gamma$  rays referred to are  $E1$ . The  $B(E1)$  values for these transitions were estimated in the same way as for  $^{144}\text{Ba}$  and are listed in Table I. They are large in absolute terms but  $B(E1; 7 \rightarrow 6)$  is significantly smaller than in  $^{144}\text{Ba}$ . This is also true for other  $B(E1)$  values since the sideways transitions from the positive-parity states to those of negative parity are too weak to be observed. The weaker

TABLE I. Electric dipole transition strengths in  $^{144}\text{Ba}$  and  $^{146}\text{Ba}$ .

$E_\gamma$ (keV)	$I_f \pi_f \rightarrow i_f \pi_i$	$I_\gamma$	$\frac{B(E1)}{B(E2)}$ <sup>a</sup>	$\frac{B(E1)}{(E1)_W}$ <sup>b</sup>
			$(10^{-6} \text{ fm}^{-2})$	
$^{144}\text{Ba}$				
317	$7^- \rightarrow 5^-$	4.3(0.9)	0.16(3)	$0.33(6) \times 10^{-3}$
394	$7^- \rightarrow 6^+$	16.5(1.5)		
509	$8^+ \rightarrow 6^+$	36.7(2.9)	1.06(34)	$2.3(7) \times 10^{-3}$
116	$8^+ \rightarrow 7^-$	2.3(0.6)		
418	$9^- \rightarrow 7^-$	15.1(1.4)	0.43(6)	$0.93(12) \times 10^{-3}$
302	$9^- \rightarrow 8^+$	18.0 (1.5)		
574	$10^+ \rightarrow 8^+$	7.2(1.1)	1.27(36)	$2.8(8) \times 10^{-3}$
272	$10^+ \rightarrow 9^-$	3.8(0.9)		
506	$11^- \rightarrow 9^-$	13.7(2.2)	0.68(18)	$1.5(4) \times 10^{-3}$
$^{146}\text{Ba}$				
204	$5^- \rightarrow 3^-$	20.0(2.8)	0.0018(3)	$4.5(8) \times 10^{-6}$
511	$5^- \rightarrow 4^+$	$4^+$	17.5(2.8)	
325	$7^- \rightarrow 5^-$	27.5(3.8)	0.0088(21)	$2.4(6) \times 10^{-5}$
390	$7^- \rightarrow 6^+$	5.0(1.3)		

<sup>a</sup> $B(E2; 2_1^+ \rightarrow 0_1^+)$  for  $^{144}\text{Ba} = 0.23 e^2$ , b<sup>2</sup>, for  $^{146}\text{Ba} = 0.29 e^2$ , b<sup>2</sup>.

<sup>b</sup> $B(E1)_W$  for  $^{144}\text{Ba} = 0.0173 e^2$ , b, for  $^{146}\text{Ba} = 0.0174 e^2$ , b. A constant quadrupole moment was assumed for each nucleus, although an increase with spin is possible.

$B(E1)$  values in  $^{146}\text{Ba}$  account for the different population patterns of the levels compared to  $^{144}\text{Ba}$ .

The level patterns in  $^{144}\text{Ba}$  and  $^{146}\text{Ba}$  are qualitatively similar to those observed in the light actinide nuclei. As the spin increases to  $\sim 8\hbar$  the level spacings approximate those of a single band, such as would arise from the rotation of an octupole-deformed shape. The differences in energy between the observed positions of the odd-parity levels and those expected for rotational bands are given by the expression

$$\delta E = E(I) - \frac{(I+1)E(I-1)^+ + IE(I+1)^+}{2I+1}$$

Figure 2 shows the quantity  $(\delta E/B)$  versus spin  $I$  for  $^{144}\text{Ba}$ ,  $^{146}\text{Ba}$ ,  $^{222}\text{Th}$ , and  $^{224}\text{Th}$ .  $B$ , the rotational constant, is deduced from the energy splittings of the  $10_1^+$  and  $8_1^+$  levels in each nucleus.

The  $B(E1)$  values for  $^{144}\text{Ba}$  given in Table I are among the largest known in medium or heavy nuclei, as are some of those measured in the neighborhood of  $^{224}\text{Th}$ . The table shows that the reduced strengths of the  $(I+1)^+ \rightarrow I^-$  transitions are somewhat larger than those of the  $I^- \rightarrow (I-1)^+$  transitions. However, with increasing spin they approach each other, as expected for a stable octupole deformation at the higher spins. Within the rotational model the  $E1$  strength may be related to an intrinsic dipole moment  $D_0$  via the expression

$$B(E1) = 3D_0^2 \langle I_f 0 | 10 | I_i 0 \rangle^2 / 4\pi.$$

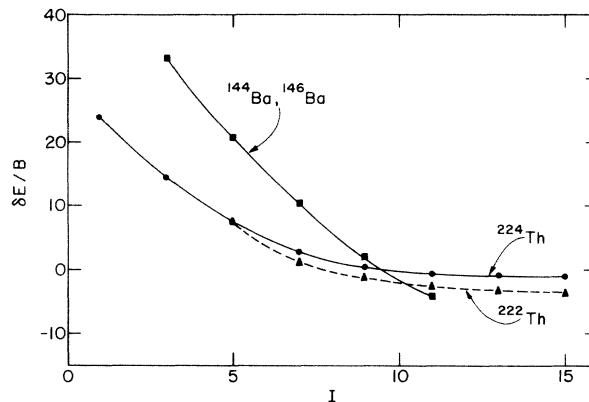


FIG. 2. The energy differences  $(\delta E/B)$  vs spin  $I$  for levels in  $^{144}\text{Ba}$ ,  $^{146}\text{Ba}$ ,  $^{222,224}\text{Th}$  (Ref. 4). The data for  $^{146}\text{Ba}$  are almost indistinguishable from those for  $^{144}\text{Ba}$  but are known up to spin  $9\hbar$  only.  $\delta E/B$  is defined in the text.

For spins  $I \gtrsim 8\hbar$  in  $^{144}\text{Ba}$  this gives an average value of  $D_0 = 0.13(1) e \cdot \text{fm}$ . On the assumption that the spin dependence of the  $E1$  transition rates in  $^{146}\text{Ba}$  is the same as in  $^{144}\text{Ba}$ , the average  $D_0$  in  $^{146}\text{Ba}$  is determined from the  $B(E1)$  for the  $7^- \rightarrow 6^+$  transition to be  $\sim 0.037 e \cdot \text{fm}$ . This is more than 3 times smaller than in  $^{144}\text{Ba}$ . The moment  $D_0$  arises from the displacements of the centers of the proton and neutron distributions from the center of mass in the asymmetric nucleus and has been written<sup>15</sup> as the sum of two components, the first calculated with the liquid-drop model and the second dependent on shell effects. The latter component may vary rapidly but smoothly with  $N$  and  $Z$ , and near  $^{224}\text{Th}$  variations in  $D_0$  are seen comparable to the difference between  $^{144}\text{Ba}$  and  $^{146}\text{Ba}$ . The spread of moments in the heavy nuclei is well described by the calculations.<sup>15</sup> Similar calculations<sup>16</sup> made recently for the Ba nuclei predict that  $D_0$  will be smaller in  $^{146}\text{Ba}$  than in  $^{144}\text{Ba}$ . These calculations predict potential surfaces which at low spin show shallow minima at an octupole deformation parameter  $\beta_3 \sim 0.1$ , which become more pronounced at higher spin. These predictions are in agreement with the observations.

Strong  $E1$  transitions are also observed<sup>17</sup> in  $^{148}\text{Sm}$  and  $^{150}\text{Sm}$  where patterns similar to those discussed in this work are seen. The calculations of Ref. 15 succeed in description of the strengths of these transitions with a dipole moment about half of those seen in the Ba or actinide region.

In summary, the present experiments show that the yrast levels of  $^{144}\text{Ba}$  and  $^{146}\text{Ba}$  are very similar in behavior to those of some light actinides. The level patterns and  $E1$  transition rates are consistent with a picture in which an octupole deformation sets in with increasing spin. The question of whether these nuclei actually acquire static octupole deformations or undergo large amplitude octupole vibrations (with an octupole-soft potential-energy surface) needs to be clarified.

We wish to thank Dr. R. R. Chasman, Dr. D. Habs, Dr. G. A. Leander, and Dr. W. Nazarewicz for helpful discussions. This research was partially supported by the U. S. Department of Energy, Nuclear Physics Division, under Contract No. W-31-109-Eng-38 and partially supported by National Science Foundation Grant No. PHY84-16025.

(a)Permanent address: Department of Physics, University of Manchester, Manchester M13 9PL, England.

(b)Permanent address: Gesellschaft für Schwerionenforschung Planckstrasse 1, D-6100, Darmstadt, Germany.

<sup>1</sup>J. Fernandez-Niello *et al.*, Nucl. Phys. **A391**, 221 (1982).

<sup>2</sup>M. Gai *et al.*, Phys. Rev. Lett. **51**, 646 (1983).

<sup>3</sup>D. Ward *et al.*, Nucl. Phys. **A406**, 591 (1983).

<sup>4</sup>P. Schüler *et al.*, Phys. Lett. **174B**, 241 (1986).

<sup>5</sup>G. A. Leander *et al.*, Nucl. Phys. **A388**, 452 (1983).

<sup>6</sup>W. Nazarewicz and P. Olanders, Nucl. Phys. **A441**, 420 (1985).

<sup>7</sup>J. Dukelsky *et al.*, Phys. Rev. C **28**, 2183 (1983).

<sup>8</sup>F. Iachello and A. D. Jackson, Phys. Lett. **108B**, 151 (1982).

<sup>9</sup>W. Nazarewicz *et al.*, Nucl. Phys. **A429**, 269 (1984).

<sup>10</sup>E. Cheifetz *et al.*, Phys. Rev. C **4**, 1913 (1971).

<sup>11</sup>S. M. Scott *et al.*, J. Phys. G **6**, 1291 (1980).

<sup>12</sup>J. B. Wilhelmy *et al.*, Phys. Rev. C **5**, 2041 (1972).

<sup>13</sup>G. Mamane *et al.*, Nucl. Phys. **A454**, 213 (1986), and references therein.

<sup>14</sup>P. M. Endt, At. Data Nucl. Data Tables **26**, 47 (1981).  
W. Andrejtscheff, K. D. Schilling, and P. Manfrass, At. Data Nucl. Data Tables **16**, 515 (1975).

<sup>15</sup>G. A. Leander *et al.*, Nucl. Phys. **A453**, 58 (1986).

<sup>16</sup>G. A. Leander and W. Nazarewicz, private communication.

<sup>17</sup>E. Hammarén *et al.*, Nucl. Phys. **A321**, 71 (1979).